Available online at www.sciencedirect.com
SCIENCE DIRECT®
Sensors and Actuators A 105 (2003) 286–292
SENSORS AND ACTUATORS A PHYSICAL
www.elsevier.com/locate/sna

# An uncooled microbolometer infrared detector based on poly-SiGe thermistor

Liang Dong*, Ruifeng Yue, Litian Liu

*Institute of Microelectronics, Tsinghua University, Beijing 100084, PR China*

Received 2 July 2002; received in revised form 15 April 2003; accepted 12 May 2003

**Abstract**

This paper reports an uncooled microbolometer infrared detector with polycrystalline silicon–germanium thermistor as the active element. Polycrystalline silicon–germanium (poly-SiGe) films are deposited by ultrahigh vacuum vapor deposition (UHV/CVD) and their structural properties are characterized by Rutherford backscattering spectrometry (RBS), SEM and Raman spectrum. The dependency of the temperature coefficient of resistance on operating temperature and on annealing temperature has been investigated. The complete fabrication of the microbolometer is described. To decrease the thermal conductance of the microbolometer, a poly-SiGe thermistor is formed on a two/four leg suspended microbridge with bulk silicon anisotropic etching and induced couple plasma (ICP) technique. Measurements and calculations show that at a bias voltage of 5 V, the maximum detectivity of $8.3 \times 10^8$ cm $Hz^{1/2}$/W is achieved at 15 Hz with a thermal response time of 16.6 ms. At a chopper frequency of 30 Hz, the maximum detectivity of $7.48 \times 10^8$ cm $Hz^{1/2}$/W and approximately 86% of the maximum responsivity are reached at 12.5 V, respectively.


*Keywords:* Microbolometer; UHV/CVD; Poly-SiGe; Infrared

## 1. Introduction

A large number of uncooled infrared focal plane arrays (IRFPA) based on a silicon IC process and a micromachining technique have been developed in the past several years [1,2]. The uncooled IRFPAs primarily include three types: microbolometer, pyroelectric and thermopile-based. We have chosen the microbolometer type detector for our present research not only because its responsivity is much higher than that of thermopile detectors, but also because it is generally easier to fabricate than pyroelectric detectors, and IR chopping is not necessary.

Important considerations when choosing the thermosensitive material for the microbolometer include a high temperature coefficient of resistance (TCR), low noise and compatibility with IC fabrication. A wide variety of materials have been used as active element for microbolometers. Vanadium oxide ($VO_x$) is the most widely used due to its high TCR of $-2$ to $-3\%\,^{\circ}C^{-1}$ and its low temperature process [1]. The main drawback of $VO_x$ is that it is not a standard material in IC fabrication processes. Although the amorphous silicon carbide ($SiC_x$) with a high TCR of $-4$ to $-6\,^{\circ}C^{-1}$ is an IC compatible material, it requires a high annealing temperature of about 1000 °C to achieve stability of microstructures, which is not suitable for post-CMOS processing since such a high temperature must have destroyed the readout circuitry [3]. Another commonly used IC compatible material is the boron doped amorphous silicon (a-Si:B) which has an attractive TCR of $-2$ to $-8\,^{\circ}C^{-1}$, while its excess low frequent noise badly compromises the TCR [4].

Since the melting point of silicon–germanium (SiGe) alloy is lower than that of Si, one advantage of polycrystalline silicon–germanium (poly-SiGe) film is that it requires lower thermal budget for crystallization, grain growth and dopant activation, thus occurring at lower temperature, than poly-Si film [5]. Additionally, the thermal conductivity of the poly-SiGe alloy is lower than that of poly-Si. For a germanium mole fraction of 30%, it is at least a factor of four lower than that of poly-Si [6–9]. In this paper, we present a microbolometer with poly-SiGe thin film resistor as thermosensitve element. Firstly, we will briefly review the theoretical consideration on responsivity and different sources of noise. Then, the deposition by ultrahigh vacuum vapor deposition (UHV/CVD) system and the structural properties of poly-SiGe will be described. After that, the microbolome-

* Corresponding author. Tel.: +86-10-62784259x320; fax: +86-10-62771130.
*E-mail address:* dongliang99@mails.tsinghua.edu.cn (L. Dong).

0924-4247/$ – see front matter © 2003 Elsevier B.V. All rights reserved.
doi:10.1016/S0924-4247(03)00232-2

ter structure and the detailed fabrication processes will be described. Finally, the performance of the microbolometer and the discussion will be presented.

## 2. Theory

The performance of a microbolometer is characterized by certain figure-of-merit such as responsivity and detectivity. The voltage responsivity $R_v$ characterizes the microbolometer response to IR radiation. It is defined as the output voltage signal divided by the input radiant power falling on the microbolometer surface, and is given by [10]:

$$R_v = \frac{|\alpha|\eta V R_b R_L}{G(R_b + R_L)^2\sqrt{1 + 4\pi^2 f^2 \tau^2}} \quad (1)$$

where $\alpha$ is the TCR defined as $\alpha = 1/R_b(\mathrm{d}R_b/\mathrm{d}T)$, $\eta$ the fraction of incident radiation absorbed, $V$ the bias voltage, $R_b$ the microbolometer resistance, $R_L$ the load resistance, $G$ the total thermal conductance to the substrate, $f$ the radiation modulation frequency and $\tau$ the thermal time constant defined by the ratio of the microbolometer's thermal mass to its thermal conductance, $C/G$. From Eq. (1) we note that the maximum responsivity is achieved for a load resistor of $R_L = R_b$.

The electrical noise is important in determining the performance of a microbolometer. The detectivity $D^*$ is a figure of merit that measures the signal-to-noise ratio and normalizes the performance of the detector with respect to the detector size, and is given by [10,11]:

$$D^* = \frac{R_v\sqrt{A_d\,\Delta f}}{V_n} \quad (2)$$

where $A_d$ is the microbolometer area, $\Delta f$ the frequent bandwidth and $V_n$ the total noise voltage of the microbolometer.

The voltage noise includes Johnson noise due to the thermal agitation of charge carriers, and $1/f$ noise observed at low frequencies usually due to trapping and detrapping mechanisms and surface state scattering. In addition, there is temperature fluctuation noise arising from the fluctuations in the heat exchange between the isolated thermosensitive element and its heat sink. The total noise voltage of the microbolometer $V_n$ is the root-mean-square of these noise components, and is given by:

$$V_n = \sqrt{\left[\left(4kT^2G\frac{R_v^2}{\eta^2}\right)^2 + 4kTR_b + \frac{C_0 I^m}{f^n}\right]\Delta f} \quad (3)$$

where $k$ is Boltzmann's constant, $T$ the working temperature, $I$ the bias current, and $C_0$, $m$ and $n$ are constants.

## 3. Deposition of the poly-SiGe film

An ultrahigh vacuum vapor deposition system was used to deposit poly-SiGe in this work, using pure silane ($SiH_4$) and germane ($GeH_4$) as the source gases. The UHV/CVD system mainly consists of a growth chamber connected to the pump system, a graphite heater around the growth chamber, a fore-chamber for loading/unloading substrates without exposing the growth chamber to air, a gas nozzle, and a transfer rod equipped with a substrate platform. A computer controls the chamber temperature and gas flow rates. The schematic diagram of the UHV/CVD system is illustrated in Fig. 1.

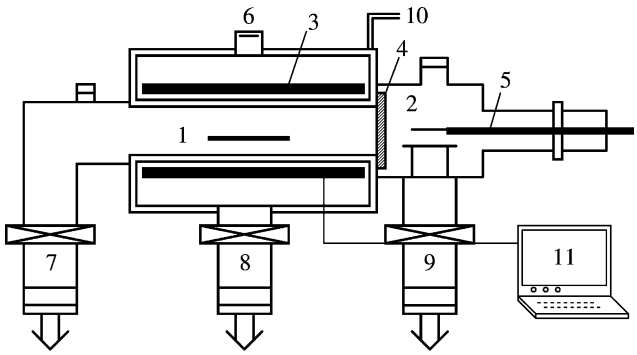


1. Growth chamber 2. Loading chamber 3. Graphite heater
4. Gate valve 5. Transfer rod 6. Pyrometer 7, 8, 9. Pumping system
10. Gas nozzle 11. Computer

Fig. 1. Schematic diagram of the UHV/CVD system.

The starting substrate was a 75 mm diameter double-side polished (1 0 0) oriented silicon wafer with 5000 Å PECVD $Si_3N_4$. The substrate was cleaned in 4:1 $H_2SO_4$:$H_2O$ at 200 °C for 20 min, followed by a deionzed water rinse and $N_2$ drying, after which it was put into the fore-chamber. When the vacuum in the fore-chamber had been pumped down rapidly to reach $10^{-5}$ Pa, the substrate was transferred into the growth chamber. Prior to deposition, the growth chamber was evacuated to a base pressure of below $1.0 \times 10^{-7}$ Pa. Deposition was carried out at a temperature of 550 °C and a chamber pressure of $2.5 \times 10^{-2}$ Pa, with flow of 15.0 sccm for $SiH_4$ and 4.4 sccm for $GeH_4$.

After deposition, poly-SiGe films were doped through ion implantation with two different boron doses: $4 \times 10^{13}$ and $5 \times 10^{15}$ $cm^{-2}$, with the same implant energy of 25 keV, and subsequently annealed at different temperatures ranging from 650 to 1050 °C for 1 min in $N_2$ ambient by rapid thermal annealing (RTA) reactor in order to investigate the effect of the annealing temperature on the resistance and TCR of poly-SiGe.

The Ge mole fraction of poly-SiGe film was determined by Rutherford backscattering spectrometry (RBS). Raman measurement was carried out using a Renishaw Raman spectrometer with the 514 nm line of an argon ion laser operated at 5 mW to avoid in situ laser annealing and damage to the samples. Sheet resistances were measured with a four-point probe.

## 4. Properties of the poly-SiGe film

RBS measurement shows that the prepared poly-SiGe film has a Ge mole fraction of 0.29, with the film thickness

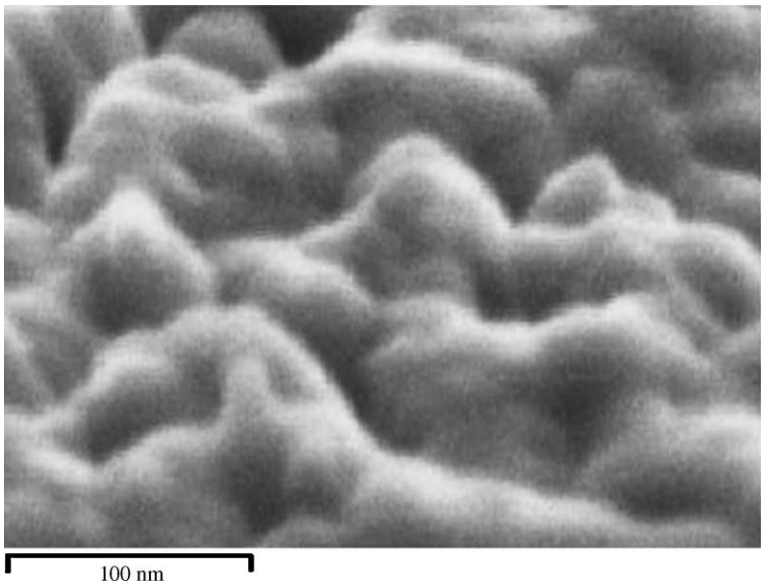


Fig. 2. SEM surface morphology of the poly-SiGe film.

of 0.5 μm. Fig. 2 is the SEM surface morphology of as-deposited poly-SiGe, indicating the formation of a polycrystalline film. The grain of poly-$Si_{0.71}Ge_{0.29}$ nestles together, with the approximate grain size of several hundreds of angstroms. Fig. 3 displays the typical Raman spectra of as-deposited poly-$Si_{0.71}Ge_{0.29}$. The three Raman peaks representing the Si–Si, Si–Ge and Ge–Ge phonon modes located at 288, 405 and 501 $cm^{-1}$, respectively, are clearly visible.

For poly-SiGe with doping dose of $4 \times 10^{13}$ $cm^{-2}$ and annealing at 650 °C, the sheet resistance ($R_s$) and calculated TCR value dependence on the operating temperature ($T$) are shown in Fig. 4. At 296 K, $R_s$ is 0.35 MΩ, and TCR is $-1.91\%$ $K^{-1}$. The $\ln R_s$, as well as the TCR, varies linearly with $1/T$. From the slope of the straight line ($\ln R_s \sim 1/T$), an activation energy of 0.145 eV can be deduced. While for film with heavily doping dose of $5 \times 10^{15}$ $cm^{-2}$ and annealing at 650 °C, $R_s$ and TCR are 0.92 kΩ and a positive value of 0.09% $K^{-1}$, respectively, indicating that such a heavy dose gives a low resistance and a negligible TCR and is suitable for electrical contacts of resistor.

Fig. 5 shows the dependence of the annealing temperature on the resistance and TCR. It is indicated that, both resistance and TCR decrease approximately linearly and not sharply until the annealing temperature reaches 950 °C, then both two drop distinctly. This may be due to the recrystallization at higher annealing temperature, forming a large crystal and reducing the total grain boundary area available to trap carriers in poly-SiGe. Thus, the activation energy must be reduced strongly, which results in a distinct drop of the resistance and TCR at 1050 °C. Fig. 5 also presents that 650 °C is enough to activate the boron dopant in poly-SiGe, which is helpful to reduce the highest temperature of microbolometer process.

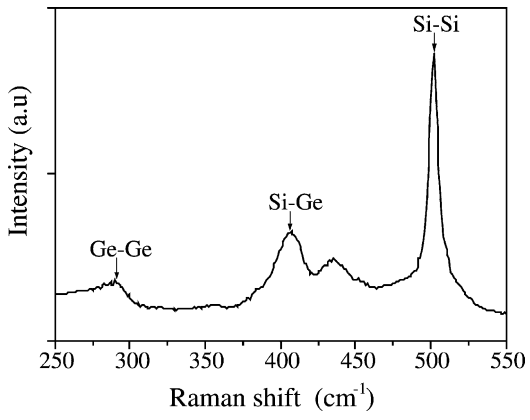


Fig. 3. Raman spectra of the poly-SiGe thin film.

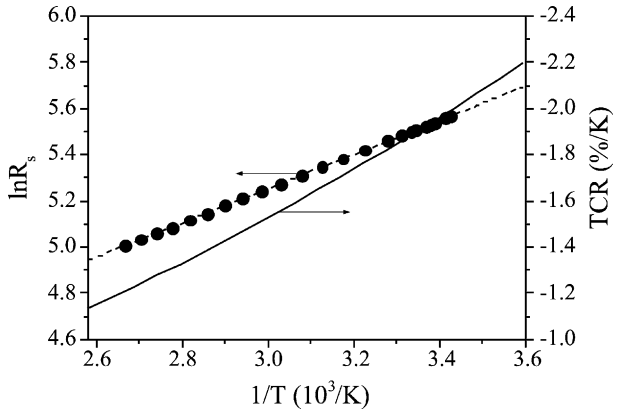


Fig. 4. Dependence of the resistance and TCR on the operating temperature.

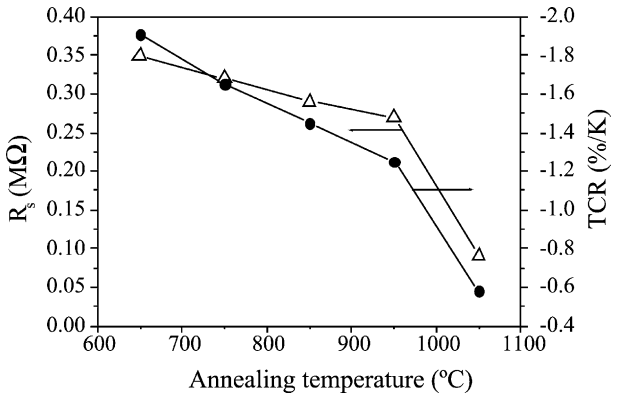


Fig. 5. Dependence of the resistance and TCR on the annealing temperature.

## 5. Microbolometer structure and fabrication

The schematic diagram of microbolometer is shown in Fig. 6. The poly-SiGe thin film resistor is located at a thermally well-isolated microbridge supported by two or four legs, which maximizes the temperature increase due to the absorption of IR radiation. The microbridge is formed by bulk micromachining. The IR absorber on the surface is a composite membrane made of $SiO_2$ and $Si_3N_4$, which can typically achieve an average absorptivity of 20–30% in the range of 8–14 μm [12].

The main fabrication process of the microbolometer is shown in Fig. 7 and can be described as follows: beginning with the 75 mm diameter double-side polished (1 0 0) oriented silicon wafers, 5000 Å thermally grown $SiO_2$ and 2000 Å LPCVD $Si_3N_4$ were used as masking layer for bulk silicon anisotropic etching. Back windows in the masking layer were patterned and opened. Wafers then were rinsed in a TMAH solution to etch a depth of 370 μm bulk silicon, leaving a silicon membrane of 30 μm. The etching details are given elsewhere [13]. In short, the etching was done at 80 °C in a 10% TMAH solution, with an etching rate of about

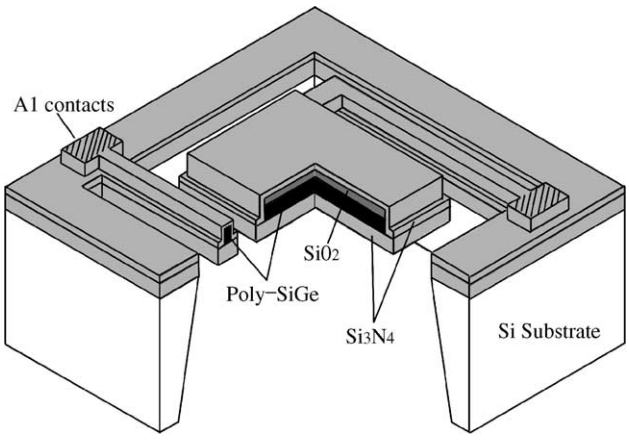


Fig. 6. Schematic diagram of the poly-SiGe microbolometer.

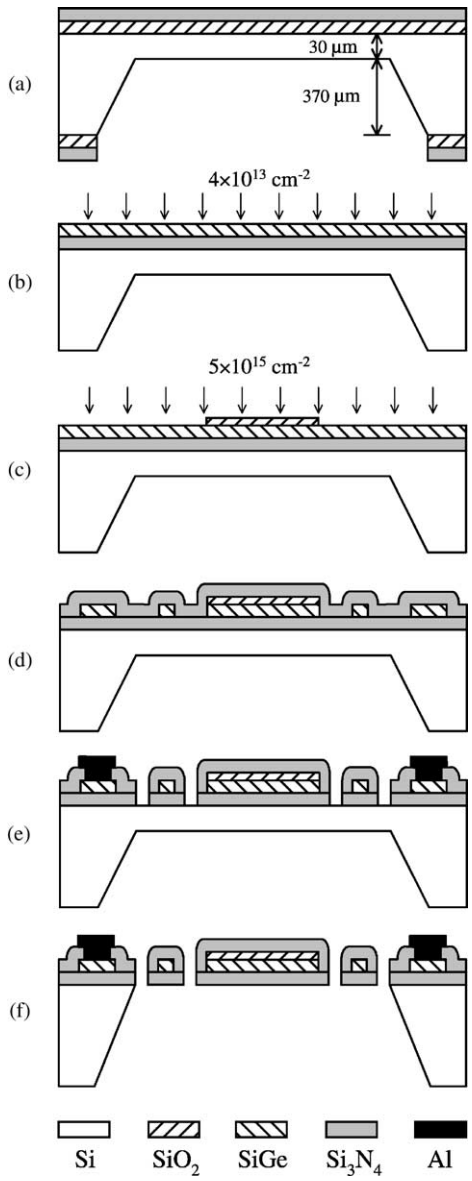


Fig. 7. Main fabrication process of the poly-SiGe microbolometer.

45 μm/h in the (1 0 0) direction (Fig. 7(a)). After the masking layers were removed, a supporting layer of 5000 Å PECVD $Si_3N_4$ and an active layer of 5000 Å UHV/CVD poly-SiGe were deposited, followed by an ion implant with a boron dose of $4 \times 10^{13}$ $cm^{-2}$ (Fig. 7(b)). Then, 2000 Å PECVD $SiO_2$ was deposited onto poly-SiGe, and was patterned to form the first layer of the IR absorber. A heavily ion implanting with a boron dose of $5 \times 10^{15}$ $cm^{-2}$ into poly-SiGe and a subsequent annealing at 650 °C for 1 min in $N_2$ ambient by RTA reactor were performed (Fig. 7(c)). The poly-SiGe was patterned to define the active area and the support legs which also act as electrical contacts. Then, 2000 Å PECVD $Si_3N_4$ was deposited as the second layer of IR absorber (Fig. 7(d)). The contacts of the electrodes were patterned and 1.0 μm aluminum was sputtered, patterned and metallized. After patterning the stack of two PECVD $Si_3N_4$, RIE technique

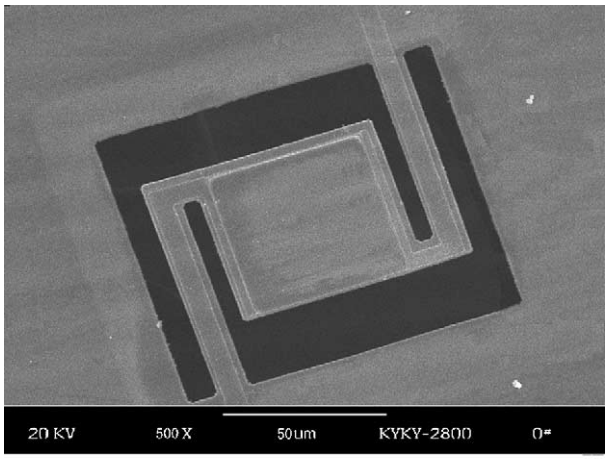


(a)

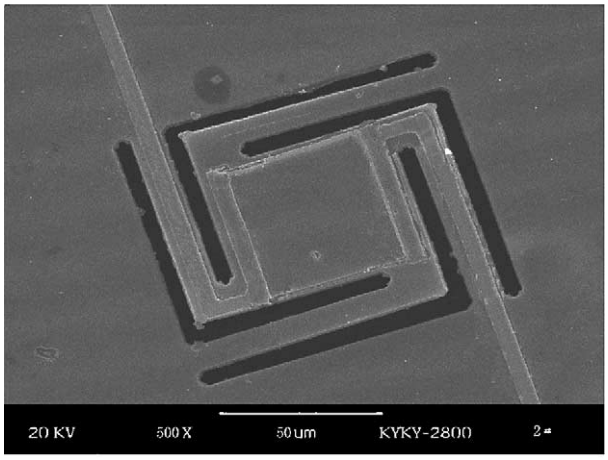


(b)

Fig. 8. SEM pictures of the poly-SiGe microbolometers with: (a) two legs or (b) four legs suspended microbridge.

was used to etch the $Si_3N_4$ layers until the top surface of the silicon appears (Fig. 7(e)). Finally, the left 30 μm silicon substrate was further etched using an induced couple plasma (ICP) system. The etchant was pure $SF_6$ gas. With a $SF_6$ flow of 6 sccm at 20 Pa and a power of 600 W during etching reaction, the silicon was etched at a rate of 1.1 μm/min (Fig. 7(f)).

Fig. 8 shows the SEM pictures of some devices with different dimensions and shapes. The structures are suspended. It should be noted here that each structure remains flat, suggesting that the stress in composite membrane is well compensated.

## 6. Characteristics and discussion

The responsivity and noise voltage of the microbolometer were measured at atmosphere pressure and an operating temperature of 296 K. The microbolometer was connected in series to a dc voltage source and to a load resistance equal

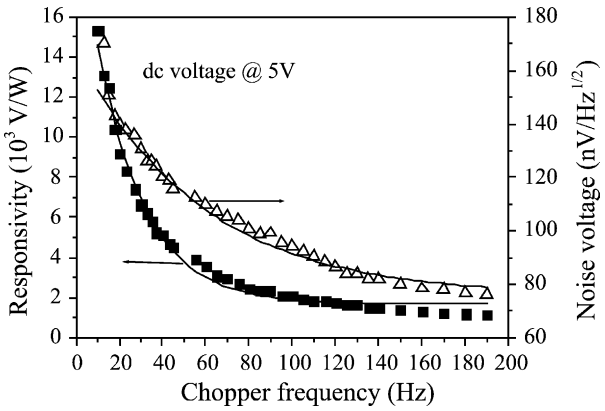


Fig. 9. Dependence of the responsivity and noise voltage on the chopper frequency.

to the microbolometer resistance. It was then exposed to the radiation of a black body at 773 K. A filter was used to reduce the spectral region of 8–14 μm. The incident radiation was modulated by a mechanical chopper, and the signal was measured using an SR510 lock-in amplifier.

Fig. 9 displays the measured responsivity and noise voltage as a function of the chopper frequency, at a bias voltage of 5 V. It is shown that poly-SiGe microbolometer has a high responsivity that depends strongly on frequency, decreasing from over 15,000 V/W at 10 Hz to about 1000 V/W at 200 Hz. The 3 dB cut-off frequency of responsivity is 60 Hz. Therefore, the thermal response time, reciprocal cut-off frequency, is approximately 16.6 ms, which is suitable for the frequency response required for 30 Hz imaging applications.

It is well known that Johnson noise voltage of per unit bandwidth, $V_J$, does not depend on the chopper frequency. For poly-SiGe microbolometer here, the calculated $V_J$ is about 45 nV/Hz$^{1/2}$. Assuming that the temperature fluctuation noise is negligible, and integrating with the measured total noise voltage shown in Fig. 9, we notice that $1/f$ noise dominates at low frequency ($f < 100$ Hz) and is comparable to Johnson noise until the chopper frequency reaches 150 Hz, and the rest is dominated by Johnson noise. The $1/f$ noise here is much higher than that in metal film microbolometer [14], while very low compared to that in amorphous silicon microbolometers [15]. The detectivity dependence on the chopper frequency, at a bias voltage of 5 V, is shown in Fig. 10, indicating the maximum detectivity of $8.3 \times 10^8$ cm Hz$^{1/2}$/W is achieved at 15 Hz.

Fig. 11 displays the responsivity and detectivity dependence on bias voltage at a chopper frequency of 30 Hz. It is clear that the responsivity first increases approximately linearly with the bias voltage, then saturates. The linear part of the curve $R_v$–$V$ in Fig. 11 is consistent with Eq. (1). To explain the saturation part, we note that the microbolometer is heated by the electrical power dissipated since it is biased using a dc voltage source. As a result, the TCR of the poly-SiGe is decreased, and then the responsivity is limited.

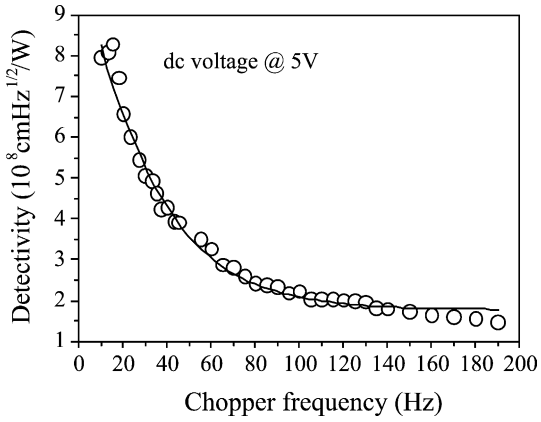


Fig. 10. Dependence of the detectivity on the chopper frequency.

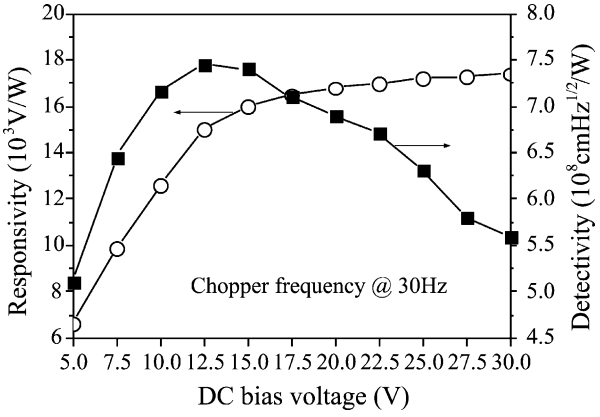


Fig. 11. Dependence of the responsivity and detectivity on the dc bias voltage.

Notice that negative slope of the curve $D^*$–$V$ in Fig. 11. As the bias voltage is increased, the $1/f$ noise dominates over the Johnson noise since $V_{1/f}$ is proportional to the bias voltage, while $V_J$ is basically invariable over the whole frequency. Therefore, at high bias voltages, the increasing $V_{1/f}$ and the simultaneously decreasing TCR badly reduce the detectivity, while at low bias voltages, the above two factors can not fully compromise the increase of the bias voltage. At the chopper frequency of 30 Hz, the maximum detectivity of $7.48 \times 10^8$ cm Hz$^{1/2}$/W and approximately 86% of the maximum responsivity of 17,400 V/W is reached at 12.5 V, respectively, so 12.5 V is considered as the optimal operating voltage.

## 7. Conclusion

We report the realization and characterization of poly-SiGe microbolometer. The ln $R_s$ and the TCR decreases linearly with the reciprocal of the operating temperature. $R_s$ and TCR vary approximately linear with annealing temperature until 950 °C is reached, when both drop distinctly. With bulk silicon anisotropic etching and ICP technique, the suspended microbridges with different shapes of support leg have been realized. In the whole procedure, 650 °C is the highest process temperature since it is enough to effectively activate the boron dopant in poly-SiGe. We have characterized the microbolometer for the infrared radiation in spectral region of 8–14 μm at an operating temperature of 296 K. It is indicated that at a bias voltage of 5 V, a maximum detectivity of $8.3 \times 10^8$ cm Hz$^{1/2}$/W at 15 Hz and a thermal response time of 16.6 ms are achieved. At a chopper frequency of 30 Hz, 12.5 V is considered as the optimal operating voltage since the maximum detectivity of $7.48 \times 10^8$ cm Hz$^{1/2}$/W and approximately 86% of the maximum responsivity of 17,400 V/W are reached, respectively.

## Acknowledgements

The authors would like to thank Prof. Yuqin Gu and Prof. Peiyi Chen for their encouragement and discussions. The work was supported by the “985” Foundation of Tsinghua University and the National Natural Science Foundation of China (No. 59995550-1).

## References

[1] R.A. Wood, Uncooled thermal imaging with monolithic silicon focal arrays, Proc. SPIE 2020 (1993) 322–329.
[2] T. Ishikawa, M. Ueno, K. Endo, Y. Nakaki, H. Hata, T. Sone, M. Kimata, T. Ozeki, Low-cost 320 × 240 uncooled IRFPA using conventional silicon IC process, Proc. SPIE 3698 (1999) 556–564.
[3] T. Ichihara, Y. Watabe, Y. Honda, K. Aizawa, A high performance amorphous $Si_{1-x}C_x$:H thermistor bolometer based on micro-machined structure, in: Proceedings of the Ninth International Conference on Solid-State Sensors and Actuators, Transducers’97, Chicago, IL, USA, 16–19 June 1997, pp. 1253–1256.
[4] J.L. Tissot, F. Rothan, C. Vedel, M. Vilain, J.J. Yon, LETI/LIR’s uncooled microbolometer development, Proc. SPIE 3379 (1998) 139–144.
[5] T.J. King, J.P. McVittie, K.C. Saraswat, J.R. Pfiester, Electrical properties of heavily doped polycrystalline silicon–germanium films, IEEE Trans. Electr. Devices 41 (2) (1994) 228–232.
[6] P.V. Gerwen, J.B. Chevrier, K. Baert, R. Mertens, T. Slater, Thin film boron-doped polycrystalline $silicon_{70\%}germanium_{30\%}$ for thermopiles, Sens. Actuators, A 53 (1996) 325–329.
[7] S. Sedky, P. Fiorini, M. Caymax, A. Verbist, C. Baert, IR bolometers made of polycrystalline silicon germanium, Sens. Actuators, A 66 (1998) 193–199.
[8] D.D.L. Wijngaards, S.H. Kong, M. Bartek, R.F. Wolffenbuttel, Design and fabrication of on-chip integrated polySiGe and polySi Peltier devices, Sens. Actuators, A 85 (2000) 316–323.
[9] M. Strasser, R. Aigner, M. Franosch, G. Wachutka, Miniaturized thermoelectric generators based on poly-Si and poly-SiGe surface micromachining, Sens. Actuators, A 97–98 (2002) 535–542.
[10] K.C. Liddiard, Thin-film resistance bolometer IR detectors, Infrared Phys. 24 (1) (1984) 57–64.
[11] M. Almasri, D.P. Butler, Z.C. Butler, Self-supporting uncooled infrared microbolometers with low-thermal mass, J. Microelectromech. Syst. 10 (3) (2001) 469–476.
[12] D. Rossberg, Optical properties of the integrated infrared sensor, in: Proceedings of the Eighth International Conference on Solid-State

Sensors and Actuators, Transducers'95, Stockholm, Sweden, 25–29 June 1995, pp. 652–655.
[13] T. Akin, Z. Olgun, O. Akar, H. Kulah, An integrated thermopile structure with high responsivity using any standard CMOS process, Sens. Actuators, A 33 (1998) 218–224.
[14] J.S. Shie, P.K. Weng, Design considerations of metal–film bolometer with micromachined floating membrane, Sens. Actuators, A 33 (1992) 182–189.
[15] T. Schimert, D. Ratcliff, J. Brady, S. Ropson, R. Gooch, B. Ritchey, P. McCardel, K. Rachels, M. Wand, M. Weinstein, J. Wynn, Low cost, low power uncooled a-Si-based micro infrared camera for unattended ground sensor applications, Proc. SPIE 3713 (1999) 101–111.

## Biographies

*Liang Dong* was born in Jiangsu Province, China, in 1976. He received the BS degree in electrical engineering from Xidian University, Xi'an, China, in 1999. He is currently working toward a PhD degree at the Institute of Microelectronics, Tsinghua University, Beijing, China. His major research interests include silicon micromachining techniques, integrated ferroelectrics-silicon devices, infrared focal plane arrays and microfluidic chips.

*Ruifeng Yue* was born in Shanxi Province, China, in 1965. He received the PhD degree from Xi'an Jiaotong University, Xi'an, China, in 1997. From 1997 to 1999, he worked as a postdoctoral research fellow at the Institute of Microelectronics, Tsinghua University. There, he is currently an associate professor. His research interests include microelectromechanical systems (MEMS), smart sensors, and microfluidic chips. He has published about 50 papers in international and domestic journals. He is also the vice director of the Device Research Division of the Institute of Microelectronics of Tsinghua University, and the senior member of China Institute of Electronics (CIE).

*Litian Liu* was born in Nanchang, China, in 1947. He graduated from the Department of Electronics Engineering, Tsinghua University, Beijing, China, in 1970. Since then he has been working on the research and development of semiconductor devices and ICs. He is currently a professor at the Institute of Microelectronics, Tsinghua University. His research fields include microelectromechanical systems (MEMS), smart sensors, bio-chips and novel semiconductor devices. Prof. Liu is the director of the Device Research Division of the Institute of Microelectronics and the vice director of the Micro/Nanometer Technology Research Center of Tsinghua University. He is also the senior member of China Institute of Electronics (CIE).